Research Square

Preprints are preliminary reports that have not undergone peer review.
They should not be considered conclusive, used to inform clinical practice,
or referenced by the media as validated information.

Noncommuting blocks in complex symmetric systems: spectral enclosures and polynomial acceleration

Raghia El hanine

elhanineraghia@gmail.com

Cadi Ayyad University

Research Article

Keywords:

Posted Date: November 17th, 2026

DOI: https://doi.org/10.21203/rs.3.rs-11579546/v1

License: This work is licensed under a Creative Commons Attribution 4.0 International License.
Read Full License

Additional Declarations: No competing interests reported.

Noncommuting blocks in complex symmetric systems: spectral enclosures and polynomial acceleration

Raghia El hanine

Laboratory LAMAI, Faculty of Sciences and Technologies,
University of Cadi Ayyad, Marrakech, Morocco

Corresponding author: elhanineraghia@gmail.com

Abstract

We analyze a relaxed block preconditioner for complex symmetric linear systems without imposing commutativity on the coefficient blocks. An explicit counterexample motivates a revised spectral analysis and demonstrates the limitations of real-spectrum conclusions in the noncommuting setting. A representation involving symmetric Cayley transforms yields corrected spectral enclosures, while commutator estimates describe how noncommutativity affects the numerical range. These estimates are used to establish convergence bounds for the generalized minimal residual method applied to the full preconditioned block system, including the contribution of block coupling. The resulting framework supports disk and Chebyshev polynomial acceleration and provides practical rules for selecting preconditioning parameters. We also derive perturbation guarantees for fixed inexact block solves, relating the accuracy of the inner computations to the resulting convergence estimates. Numerical experiments on dense and sparse test problems examine the spectral enclosures and polynomial bounds and compare the computational work required by different polynomial degrees. The results quantify the tradeoff between fewer outer Krylov iterations and additional preconditioner applications, providing guidance for choosing polynomial degrees and assessing the computational benefits of polynomial acceleration.

Keywords: complex symmetric systems; block preconditioning; noncommuting matrices; Cayley transforms; numerical range; polynomial acceleration.
MSC 2020: 65F08, 65F10, 65F15.

1 Introduction

Complex symmetric systems arise in frequency-domain models and many other scientific computations. Their real representations often expose useful two-by-two block structure. Splitting preconditioners exploit this structure by replacing one difficult complex solve with simpler real subproblems. The Hermitian and skew-Hermitian splitting framework of Bai, Golub and Ng [1] is a fundamental example. Zhang and Dai [11] introduced a relaxed block preconditioner that requires two symmetric positive definite (SPD) subsolves even when the real part of the original complex coefficient matrix is indefinite. Subsequent modifications include the matrix-parameter approach of Bao and Miao [2]. Recent block-splitting developments also investigate convergence and spectral properties for complex symmetric systems [10].

Spectral analysis is especially delicate when symmetric blocks do not commute. Products of positive definite matrices need not be symmetric, and the positive spectrum of a product does not imply positivity of all its quadratic forms. Moreover, eigenvalue localization alone does not determine GMRES convergence; see [7]. This motivates estimates based on operator norms and numerical ranges. General polynomial bounds follow from the numerical-range inequality

of Crouzeix and Palencia [5]; extensions and applications to Krylov methods are discussed in [4, 3]. Weighted inner products can reveal additional structure [6].

This paper develops a spectral and polynomial analysis of the relaxed preconditioner in [11] when its blocks do not commute. An explicit counterexample first establishes the need to revise the real-interval conclusion of its Theorem 1. A Cayley-transform representation then yields a disk enclosure and commutator-dependent bounds for the numerical range. These bounds remain valid for a singular symmetric block. A block-polynomial identity transfers reduced estimates to the full system while accounting explicitly for the coupling block and the unit eigenvalues. Combining this identity with disk polynomials or Chebyshev polynomials on enclosing ellipses produces a polynomial approximate inverse with a computable error bound. The analysis also gives a two-candidate parameter rule and a perturbation guarantee for fixed linear inexact block solves.

The construction uses established Cayley-transform, polynomial approximation and spectral-set principles. Its purpose is to provide quantitative bounds for this block structure, including terms that spectral localization alone does not control. The numerical experiments examine the resulting spectral geometry, polynomial bounds and computational work. Preconditioner actions and orthogonalization operations are reported separately so that a reduction in outer iterations can be assessed against the work required to obtain it.

The paper is organized as follows. Section 2 gives the block reduction and counterexample. Section 3 establishes the spectral and numerical-range bounds, and Section 4 derives full-system convergence estimates. Polynomial acceleration, inexact solves and parameter selection are treated in Sections 5–7. Section 8 presents the numerical experiments.

All norms without a subscript are the matrix or vector Euclidean 2-norm. For a real matrix, the numerical range is taken over complex vectors:

$$\mathcal{W}(X) = \{v^* X v : v \in \mathbb{C}^n,\ v^* v = 1\}.$$

We use $[X, Y] = XY - YX$, $\mathrm{sym}(X) = (X + X^T)/2$ and $\mathrm{skew}(X) = (X - X^T)/2$.

2 Block reduction and a counterexample

Let $T, W \in \mathbb{R}^{n\times n}$ satisfy

$$T = T^T \succ 0, \qquad W = W^T. \tag{2.1}$$

The indefinite case is the motivating setting, but the results below do not require W to have both positive and negative eigenvalues. Consider

$$\mathcal{A} = \begin{pmatrix} T & -W \\ W & T \end{pmatrix}, \qquad \mathcal{P}_\alpha = \begin{pmatrix} \alpha I + T & -W \\ W(I + \alpha^{-1} T) & T \end{pmatrix}, \qquad \alpha > 0. \tag{2.2}$$

The complex symmetric system

$$(W + iT)(u + iv) = f + ig$$

is equivalent to $\mathcal{A}x = b$ with $x = (u^T, -v^T)^T$ and $b = (g^T, f^T)^T$. The symmetric part of $\mathcal{A}$ is $\mathrm{diag}(T, T) \succ 0$, so $\mathcal{A}$ is nonsingular. We set

$$S_\alpha = \alpha I + T, \qquad H_\alpha = T + \alpha^{-1} W^2, \qquad U = W T^{-1} W \succeq 0. \tag{2.3}$$

Both S_α and H_α are SPD.

Lemma 2.1. *The action of $\mathcal{P}_\alpha^{-1}$ is well defined and can be computed by*

$$z_2 = H_\alpha^{-1}(r_2 - \alpha^{-1} W r_1), \tag{2.4}$$

$$z_1 = S_\alpha^{-1}(r_1 + W z_2). \tag{2.5}$$

Moreover,

$$\mathcal{B}_\alpha := \mathcal{P}_\alpha^{-1}\mathcal{A} = \begin{pmatrix} E_\alpha & 0 \\ F_\alpha & I \end{pmatrix}, \tag{2.6}$$

where

$$E_\alpha = \alpha S_\alpha^{-1}(\alpha I + U)^{-1}(U + T), \tag{2.7}$$
$$F_\alpha = H_\alpha^{-1}W(I - \alpha^{-1}T). \tag{2.8}$$

These identities hold when W is singular.

Proof. The second block row of $\mathcal{P}_\alpha z = r$ contains $\alpha^{-1}WS_\alpha z_1 + Tz_2 = r_2$. Substitution of $S_\alpha z_1 = r_1 + Wz_2$ gives (2.4) and (2.5). The two SPD solves also prove nonsingularity. For $r = \mathcal{A}(x_1, x_2)^T$, these formulas give $z_2 = F_\alpha x_1 + x_2$ and $z_1 = S_\alpha^{-1}(T + WF_\alpha)x_1$.

The Woodbury identity, applied using the nonsingular matrices T and $\alpha I + U$, gives

$$H_\alpha^{-1} = T^{-1} - T^{-1}W(\alpha I + U)^{-1}WT^{-1}.$$

Consequently

$$WH_\alpha^{-1}W = U - U(\alpha I + U)^{-1}U = \alpha U(\alpha I + U)^{-1}. \tag{2.9}$$

Substitution into $S_\alpha^{-1}(T + WF_\alpha)$ yields (2.7), without invoking W^{-1}. □

Example 2.2 (A nonreal pair under the stated symmetry assumptions)**.** Take $n = 2$, $\alpha = 1$, and

$$T = \begin{pmatrix} 1/2 & 0 \\ 0 & 2 \end{pmatrix}, \qquad W = \begin{pmatrix} 0 & 1 \\ 1 & 1 \end{pmatrix}.$$

The matrix T is SPD and $\det W = -1$, so W is symmetric indefinite. Direct rational arithmetic gives

$$\mathcal{P}_1^{-1}\mathcal{A} = \begin{pmatrix} 13/30 & -1/15 & 0 & 0 \\ 1/60 & 13/30 & 0 & 0 \\ -1/10 & -3/5 & 1 & 0 \\ 3/20 & -1/10 & 0 & 1 \end{pmatrix}.$$

Its characteristic polynomial is

$$\frac{(\lambda - 1)^2(90\lambda^2 - 78\lambda + 17)}{90},$$

and hence

$$\sigma(\mathcal{P}_1^{-1}\mathcal{A}) = \left\{1, \frac{13 + i}{30}, \frac{13 - i}{30}\right\}. \tag{2.10}$$

Thus the real-interval conclusion in Theorem 1 of [11] does not hold under those hypotheses alone. The example concerns the spectral statement, not the practical effectiveness of the preconditioner.

3 Cayley transforms, commutators and numerical ranges

For a symmetric positive semidefinite X, define

$$C_\alpha(X) = (\alpha I - X)(\alpha I + X)^{-1}, \qquad \vartheta_\alpha(X) = \|C_\alpha(X)\|_2 = \max_{\lambda \in \sigma(X)} \left|\frac{\alpha - \lambda}{\alpha + \lambda}\right|. \tag{3.1}$$

The matrix $C_\alpha(X)$ is symmetric, with norm at most 1; the inequality is strict if X is positive definite. Write

$$\widehat{E}_\alpha = S_\alpha E_\alpha S_\alpha^{-1}, \qquad q_\alpha = \vartheta_\alpha(U)\vartheta_\alpha(T) < 1. \tag{3.2}$$

Theorem 3.1 (Corrected disk enclosure)**.** *Under* (2.1)*, for every* $\alpha > 0$*,*

$$\widehat{E}_\alpha = \frac{1}{2}(I - C_\alpha(U)C_\alpha(T)). \tag{3.3}$$

In particular,

$$\left\| I - 2\widehat{E}_\alpha \right\|_2 \le q_\alpha < 1, \tag{3.4}$$

and

$$\sigma(\mathcal{B}_\alpha) \subset \{1\} \cup \left\{ z \in \mathbb{C} : \left| z - \frac{1}{2} \right| \le \frac{q_\alpha}{2} \right\}. \tag{3.5}$$

Every nonunit eigenvalue has positive real part and modulus strictly less than 1.

Proof. Expanding the products in

$$(\alpha I + U)(\alpha I + T) - (\alpha I - U)(\alpha I - T) = 2\alpha(U + T)$$

and multiplying on the left by $(\alpha I + U)^{-1}$ and on the right by $(\alpha I + T)^{-1}$ proves (3.3) using (2.7). Submultiplicativity proves (3.4). Since $\vartheta_\alpha(U) \le 1$ and $\vartheta_\alpha(T) < 1$, their product is strictly below 1. The eigenvalue enclosure follows from $\sigma(\mathcal{B}_\alpha) = \sigma(E_\alpha) \cup \{1\}$ and similarity. □

Proposition 3.2 (Two sufficient conditions for a real spectrum)**.** *The matrix* $\widehat{E}_\alpha$ *is symmetric if and only if* $[U, T] = 0$*. In this case its eigenvalues belong to* $[(1 - q_\alpha)/2, (1 + q_\alpha)/2]$*. The eigenvalues of* $\widehat{E}_\alpha$ *are also real if*

$$0 < \alpha < \lambda_{\min}(T) \quad \text{or} \quad \alpha > \lambda_{\max}(T),$$

without a commutativity assumption.

Proof. By (3.3), symmetry is equivalent to $[C_\alpha(U), C_\alpha(T)] = 0$. The Cayley transforms commute if U, T commute. Conversely, $C_\alpha(X) = 2\alpha(\alpha I + X)^{-1} - I$; commutativity of the transforms implies commutativity of the resolvents, their inverses and hence U, T. The interval follows from theorem 3.1.

Under either strict inequality on α, $C_\alpha(T) = sJ$, where $s \in \{-1, 1\}$ and $J \succ 0$. Then

$$J^{1/2}(C_\alpha(U)C_\alpha(T))J^{-1/2} = sJ^{1/2}C_\alpha(U)J^{1/2}$$

is symmetric. The product and $\widehat{E}_\alpha$ therefore have real spectra. □

Remark 3.3. The commutator relevant to the reduced block is $[U, T]$, rather than only $[W, T]$. For example, if $W = \left(\begin{smallmatrix} 0 & 1 \\ 1 & 0 \end{smallmatrix}\right)$ and $T = \operatorname{diag}(t_1, t_2)$ with distinct positive t_1, t_2, then $[W, T] \neq 0$ but $U = \operatorname{diag}(t_2^{-1}, t_1^{-1})$ commutes with T. Conversely, a real spectrum need not imply symmetry, as proposition 3.2 also shows.

Theorem 3.4 (Commutator-dependent enclosure)**.** *Set* $c = 1/2$ *and*

$$a_\alpha = \left\| \operatorname{sym}(\widehat{E}_\alpha) - cI \right\|_2, \tag{3.6}$$

$$b_\alpha = \left\| \operatorname{skew}(\widehat{E}_\alpha) \right\|_2 = \frac{1}{4} \left\| [C_\alpha(U), C_\alpha(T)] \right\|_2. \tag{3.7}$$

Then $a_\alpha \le q_\alpha/2$*,* $b_\alpha \le q_\alpha/2$*, and*

$$\mathcal{W}(\widehat{E}_\alpha) \subset \{ z : |\operatorname{Re} z - c| \le a_\alpha,\ |\operatorname{Im} z| \le b_\alpha \}. \tag{3.8}$$

If $u_- = \lambda_{\min}(U)$ *and* $t_- = \lambda_{\min}(T)$*, then*

$$b_\alpha \le \frac{\alpha^2 \left\| [U, T] \right\|_2}{(\alpha + u_-)^2(\alpha + t_-)^2}. \tag{3.9}$$

Furthermore,

$$[U,T] = WT^{-1}[W,T] + [W,T]T^{-1}W, \qquad \|[U,T]\|_2 \le 2\,\|W\|_2 \left\|T^{-1}\right\|_2 \|[W,T]\|_2\,. \tag{3.10}$$

The departure from normality satisfies

$$\left\|\widehat{E}_\alpha \widehat{E}_\alpha^T - \widehat{E}_\alpha^T \widehat{E}_\alpha\right\|_2 \le 4a_\alpha b_\alpha. \tag{3.11}$$

Proof. Taking the transpose of (3.3) proves (3.7). The norms of the symmetric and skew-symmetric parts of $\widehat{E}_\alpha - cI$ are bounded by $\left\|\widehat{E}_\alpha - cI\right\|_2 \le q_\alpha/2$. For a complex unit vector v, $v^*\,\mathrm{sym}(\widehat{E}_\alpha)v$ is real and $v^*\,\mathrm{skew}(\widehat{E}_\alpha)v$ is purely imaginary; their magnitudes prove (3.8).

Let $R_U = (\alpha I + U)^{-1}$ and $R_T = (\alpha I + T)^{-1}$. The inverse-commutator identity gives

$$[C_\alpha(U), C_\alpha(T)] = 4\alpha^2 R_U R_T [U,T] R_T R_U.$$

Its norm proves (3.9). Expanding the right-hand side of (3.10) proves the identity and then its norm estimate. Finally write $\widehat{E}_\alpha = cI + J + K$, with $J = J^T$, $K = -K^T$, $\|J\|_2 = a_\alpha$, and $\|K\|_2 = b_\alpha$. The commutator with the transpose is $2(KJ - JK)$, which proves (3.11). □

Remark 3.5 (Bounds versus estimates). All enclosure theorems remain valid if $q_\alpha, a_\alpha, b_\alpha$ are replaced by proven upper bounds, with $q_\alpha < 1$ retained. For example, (3.9)–(3.10) and $\|X\|_2 \le \sqrt{\|X\|_1 \|X\|_\infty}$ give conservative computable bounds when lower spectral bounds for T are known. Lanczos or randomized norm estimates are useful diagnostics, but without an additional certification step they are not guaranteed upper bounds. The dense experiments below use explicitly assembled matrices and numerical norms.

4 Residual-polynomial estimates for the full block system

The unit eigenvalues in (2.6) require separate treatment from the reduced block. Let

$$D_\alpha = \mathrm{diag}(S_\alpha, I), \qquad \widehat{\mathcal{B}}_\alpha = D_\alpha \mathcal{B}_\alpha D_\alpha^{-1} = \begin{pmatrix} \widehat{E}_\alpha & 0 \\ G_\alpha & I \end{pmatrix}, \quad G_\alpha = F_\alpha S_\alpha^{-1}. \tag{4.1}$$

Define the explicit upper bound

$$\Gamma_\alpha = \sqrt{\left(\frac{1+q_\alpha}{2}\right)^2 + \|G_\alpha\|_2^2}. \tag{4.2}$$

Theorem 4.1 (Transfer of reduced polynomial estimates)**.** *Let h be a polynomial with $h(0) = 1$, and set $p(z) = (1-z)h(z)$. Then*

$$p(\widehat{\mathcal{B}}_\alpha) = \begin{pmatrix} (I - \widehat{E}_\alpha)h(\widehat{E}_\alpha) & 0 \\ -G_\alpha h(\widehat{E}_\alpha) & 0 \end{pmatrix}, \tag{4.3}$$

and

$$\left\|p(\widehat{\mathcal{B}}_\alpha)\right\|_2 \le \Gamma_\alpha \left\|h(\widehat{E}_\alpha)\right\|_2. \tag{4.4}$$

Consequently, for unrestarted GMRES on $\widehat{\mathcal{B}}_\alpha y = \widehat{f}$, $k \ge 1$ implies

$$\frac{\|\widehat{r}_k\|_2}{\|\widehat{r}_0\|_2} \le \min\{1, \Gamma_\alpha q_\alpha^{k-1}\}. \tag{4.5}$$

For unrestarted GMRES on the reduced system $\widehat{E}_\alpha v = g$, the corresponding bound is q_α^k.

Proof. The top row of $h(\widehat{\mathcal{B}}_\alpha)$ is $(h(\widehat{E}_\alpha), 0)$. Multiplication on the left by $I - \widehat{\mathcal{B}}_\alpha = \begin{pmatrix} I-\widehat{E}_\alpha & 0 \\ -G_\alpha & 0 \end{pmatrix}$ proves (4.3). Also

$$\left\| I - \widehat{E}_\alpha \right\|_2 = \frac{1}{2} \left\| I + C_\alpha(U) C_\alpha(T) \right\|_2 \le \frac{1 + q_\alpha}{2},$$

so the norm of the block column in (4.3) is at most Γ_α. This proves (4.4).

The GMRES minimum-residual characterization [9] bounds the residual by any polynomial of degree at most k with value 1 at zero. Choose $h(z) = (1-2z)^{k-1}$ and use (3.4). The reduced bound uses $(1-2z)^k$. The constant polynomial 1 supplies the other term in the minimum. □

Corollary 4.2 (Restarted and unscaled forms)**.** *For GMRES restarted every $r \ge 1$ steps on the scaled system, if $\rho_r := \Gamma_\alpha q_\alpha^{r-1} < 1$, then*

$$\|\widehat{r}_{jr}\|_2 \le \rho_r^j \|\widehat{r}_0\|_2, \qquad j = 0, 1, \ldots.$$

For Euclidean GMRES on $\mathcal{B}_\alpha x = f$, the bound (4.5) holds with Γ_α replaced by $\kappa_2(D_\alpha)\Gamma_\alpha$.

Proof. Apply the polynomial estimate to the residual at each restart. For the unscaled system, use $p(\mathcal{B}_\alpha) = D_\alpha^{-1} p(\widehat{\mathcal{B}}_\alpha) D_\alpha$ in the minimum-residual characterization. □

Remark 4.3 (Physical residuals and mesh independence). The scaled right-hand side for $\mathcal{A}x = b$ is $\widehat{f} = D_\alpha \mathcal{P}_\alpha^{-1} b$, with $y = D_\alpha x$. Hence

$$\widehat{r} = D_\alpha \mathcal{P}_\alpha^{-1}(b - \mathcal{A}x), \qquad \|b - \mathcal{A}x\|_2 \le \left\| \mathcal{P}_\alpha D_\alpha^{-1} \right\|_2 \|\widehat{r}\|_2 .$$

A relative physical-residual estimate therefore includes $\kappa_2(\mathcal{P}_\alpha D_\alpha^{-1})$. Dimension-independent spectral enclosures alone do not establish mesh-independent convergence in every norm. Uniform control of the relevant coupling and norm-equivalence constants is needed. In experiments we check the physical residual explicitly.

5 Commutator-dependent Chebyshev acceleration

5.1 Enclosing ellipses

Use bounds $a \ge a_\alpha$, $b \ge b_\alpha$ from theorem 3.4. A horizontal ellipse centered at $c = 1/2$ is

$$\mathcal{E}(A, B) = \left\{ x + iy : \frac{(x-c)^2}{A^2} + \frac{y^2}{B^2} \le 1 \right\}, \qquad 0 < B < A < c.$$

If

$$\frac{a^2}{A^2} + \frac{b^2}{B^2} \le 1, \tag{5.1}$$

then the rectangle in (3.8) lies in $\mathcal{E}(A, B)$. For $b > 0$, a convenient one-parameter construction is

$$\sqrt{a^2 + b^2} < A < c, \qquad B = \frac{b}{\sqrt{1 - a^2/A^2}}. \tag{5.2}$$

It has $B < A$, contains the rectangle, and excludes the origin. If the interval for A is empty, this construction is unavailable and the disk polynomial below remains valid. The construction need not be the tightest ellipse containing the intersection of the rectangle and Cayley disk.

Let

$$d = \sqrt{A^2 - B^2}, \quad \rho = \frac{A + B}{d}, \quad \tau = \frac{c}{d} + \sqrt{\left(\frac{c}{d}\right)^2 - 1}. \tag{5.3}$$

Then $1 < \rho < \tau$. For the Chebyshev polynomial T_ℓ of the first kind, define

$$h_\ell^{\mathrm{ell}}(z) = \frac{T_\ell((c-z)/d)}{T_\ell(c/d)}, \qquad \ell \ge 0. \tag{5.4}$$

Its value at zero is 1, and the denominator is strictly positive.

Theorem 5.1 (Ellipse polynomial bound)**.** *Assume* (5.1) *and* $0 < B < A < c$*. For* $\ell \geq 1$*,*

$$\left\| h_\ell^{\mathrm{ell}}(\widehat{E}_\alpha) \right\|_2 \leq \Theta_\ell^{\mathrm{ell}} := (1+\sqrt{2}) \frac{\rho^\ell + \rho^{-\ell}}{\tau^\ell + \tau^{-\ell}} \leq 2(1+\sqrt{2})(\rho/\tau)^\ell. \tag{5.5}$$

If $b_\alpha = 0$*,* $\widehat{E}_\alpha$ *is symmetric and the interval polynomial*

$$h_\ell^{\mathrm{int}}(z) = \frac{T_\ell((c-z)/a)}{T_\ell(c/a)}, \qquad 0 < a < c,$$

satisfies

$$\left\| h_\ell^{\mathrm{int}}(\widehat{E}_\alpha) \right\|_2 \leq \frac{1}{T_\ell(c/a)}. \tag{5.6}$$

Proof. The boundary of the ellipse can be parametrized so that $(c-z)/d = (w + w^{-1})/2$ with $|w| = \rho$. The identity $T_\ell((w + w^{-1})/2) = (w^\ell + w^{-\ell})/2$ gives

$$\max_{z \in \mathcal{E}(A,B)} |T_\ell((c-z)/d)| \leq (\rho^\ell + \rho^{-\ell})/2.$$

Also $T_\ell(c/d) = (\tau^\ell + \tau^{-\ell})/2$. The Crouzeix–Palencia inequality [5], applied to $\widehat{E}_\alpha$ and its numerical range, proves the first bound. The second follows from $\rho^\ell + \rho^{-\ell} \leq 2\rho^\ell$ and $\tau^\ell + \tau^{-\ell} \geq \tau^\ell$. For $b_\alpha = 0$, the spectral theorem applies directly and the interval bound follows from $|T_\ell(t)| \leq 1$ on $[-1, 1]$. □

For comparison define the disk polynomial and bound

$$h_\ell^{\mathrm{disk}}(z) = (1-2z)^\ell, \qquad \Theta_\ell^{\mathrm{disk}} = q_\alpha^\ell. \tag{5.7}$$

At each chosen degree, select whichever available construction has the smaller proven bound. For $\ell = 0$, take $h_0 = 1$ and $\Theta_0 = 1$. Let h_ℓ denote the selected polynomial and Θ_ℓ its bound.

5.2 A polynomial approximate inverse

Define

$$p_{\ell+1}(z) = (1-z)h_\ell(z), \qquad \psi_\ell(z) = \frac{1 - p_{\ell+1}(z)}{z}. \tag{5.8}$$

Since $p_{\ell+1}(0) = 1$, ψ_ℓ is a polynomial of degree at most ℓ. There is no division by a matrix in its implementation.

Theorem 5.2 (Polynomial preconditioning)**.** *Let* $\mathcal{Q}_\ell = \psi_\ell(\mathcal{B}_\alpha)\mathcal{P}_\alpha^{-1}$ *and* $\epsilon_\ell = \Gamma_\alpha \Theta_\ell$*. Then*

$$\left\| I - D_\alpha \mathcal{Q}_\ell \mathcal{A} D_\alpha^{-1} \right\|_2 \leq \epsilon_\ell. \tag{5.9}$$

If $\epsilon_\ell < 1$*,* $\mathcal{Q}_\ell$ *is nonsingular and unrestarted GMRES on* $D_\alpha \mathcal{Q}_\ell \mathcal{A} D_\alpha^{-1}$ *has relative residual at most* ϵ_ℓ^k *after* k *steps. The same bound applies to the right-polynomial-preconditioned scaled matrix* $\widehat{\mathcal{B}}_\alpha \psi_\ell(\widehat{\mathcal{B}}_\alpha)$*.*

Proof. Polynomial commutativity and (5.8) give

$$\mathcal{Q}_\ell \mathcal{A} = \psi_\ell(\mathcal{B}_\alpha)\mathcal{B}_\alpha = I - p_{\ell+1}(\mathcal{B}_\alpha).$$

Use similarity, theorem 4.1, and the selected reduced bound. If $\epsilon_\ell < 1$, the matrix on the left is invertible by the Neumann series. Since $\mathcal{A}$ is invertible, so is $\mathcal{Q}_\ell$. The residual polynomial $(1-z)^k$ gives the GMRES estimate. □

For a target $0 < \varepsilon < 1$, a certified degree is

$$\ell_* = \min\{\ell \geq 0 : \Gamma_\alpha \Theta_\ell \leq \varepsilon\}. \tag{5.10}$$

The disk branch ensures existence. If $0 < q_\alpha < 1$, the conservative disk choice is any integer satisfying $\ell \geq \max\{0, \log(\varepsilon/\Gamma_\alpha)/\log q_\alpha\}$. If $q_\alpha = 0$, degree 1 already annihilates the reduced block.

5.3 Matrix-free recurrence and work

For the ellipse, put $t_j = T_j(c/d)$. The normalized recurrence is

$$A_j = \frac{2t_j}{dt_{j+1}}, \qquad B_j = \frac{t_{j-1}}{t_{j+1}}, \qquad h_{j+1}(z) = A_j(c-z)h_j(z) - B_j h_{j-1}(z). \tag{5.11}$$

The identity $A_j c - B_j = 1$ preserves normalization at zero. Let $s_j(z) = (1 - h_j(z))/z$. Then

$$s_{j+1} = A_j c\, s_j - B_j s_{j-1} + A_j h_j, \qquad \psi_j = h_j + s_j. \tag{5.12}$$

These formulas give algorithm 5.3. Evaluate the ratios t_j/t_{j+1} using $\log\cosh(j \operatorname{arcosh}(c/d))$ when direct evaluation risks overflow.

Algorithm 5.3 (Apply $\psi_\ell(B)v$ for a fixed ellipse polynomial)**.** Given a matrix action $w \mapsto Bw$, vector v, degree ℓ and ellipse parameters, perform the following steps.

1. If $\ell = 0$, return v.
2. Set $h_0 = v$, $s_0 = 0$, $h_1 = v - Bv/c$ and $s_1 = v/c$.
3. For $j = 1, \dots, \ell - 1$, compute A_j, B_j from (5.11) and set
$$h_{j+1} = A_j(ch_j - Bh_j) - B_j h_{j-1}, \qquad s_{j+1} = A_j c\, s_j - B_j s_{j-1} + A_j h_j.$$
4. Return $h_\ell + s_\ell$.

For the disk branch, start with $h = v$, $s = 0$ and repeat

$$s \leftarrow s + 2h, \qquad h \leftarrow h - 2Bh$$

ℓ times, using the old h in both updates; return $h + s$. Both recurrences use exactly ℓ actions of B and no inner products. Applying $\mathcal{Q}_\ell$ requires one additional $\mathcal{P}_\alpha^{-1}$ action. The total is $\ell + 1$ preconditioner applications and ℓ applications of $\mathcal{A}$, plus vector operations. The polynomial does not remove work from its constituent matrix or preconditioner actions. Its potential advantage is reduced outer orthogonalization and memory use.

6 Fixed linear inexact block solves

Let M_S and M_H be fixed linear approximations to S_α^{-1} and H_α^{-1}. Using them in (2.4)–(2.5) defines a fixed linear map $\widetilde{M}$. Set

$$\widetilde{\mathcal{B}} = \widetilde{M}\mathcal{A}, \qquad \widetilde{\widehat{\mathcal{B}}} = D_\alpha \widetilde{\mathcal{B}} D_\alpha^{-1}.$$

The right-hand side is preconditioned by the same map. This consistency is essential: a fixed approximate inverse is used as a preconditioner for the original system, rather than replacing its coefficient matrix.

Lemma 6.1 (From inner errors to a preconditioner error)**.** *Let* $e_S = \|M_S - S_\alpha^{-1}\|_2$, $e_H = \|M_H - H_\alpha^{-1}\|_2$, $w = \|W\|_2$, *and* $L = \sqrt{1 + \alpha^{-2}w^2}$. *Then*

$$\left\|\widetilde{M} - \mathcal{P}_\alpha^{-1}\right\|_2 \le e_S(1 + w\left\|H_\alpha^{-1}\right\|_2 L) + e_H L\sqrt{1 + \|M_S W\|_2^2} =: \zeta, \tag{6.1}$$

$$\left\|\widetilde{\widehat{\mathcal{B}}} - \widehat{\mathcal{B}}_\alpha\right\|_2 \le \|D_\alpha\|_2 \left\|\mathcal{A}D_\alpha^{-1}\right\|_2 \zeta =: \eta. \tag{6.2}$$

Proof. Let $J = (I, 0)$, $L_0 = (-\alpha^{-1}W, I)$, $E_S = M_S - S_\alpha^{-1}$ and $E_H = M_H - H_\alpha^{-1}$. Subtracting the exact and approximate block formulas gives

$$\widetilde{M} - \mathcal{P}_\alpha^{-1} = \begin{pmatrix} E_S J + E_S W H_\alpha^{-1} L_0 \\ 0 \end{pmatrix} + \begin{pmatrix} M_S W \\ I \end{pmatrix} E_H L_0.$$

Since $\|L_0\|_2 = L$ and $\left\| \left(\begin{smallmatrix} M_S W \\ I \end{smallmatrix}\right) \right\|_2 = \sqrt{1 + \|M_S W\|_2^2}$, (6.1) follows. Multiplication by D_α and $\mathcal{A}D_\alpha^{-1}$ proves (6.2). □

If M_X is a polynomial approximate inverse of an SPD matrix X and $\max_{\lambda \in \sigma(X)} |1 - \lambda M_X(\lambda)| \le \delta_X$, then

$$\left\| M_X - X^{-1} \right\|_2 \le \delta_X / \lambda_{\min}(X). \tag{6.3}$$

In particular, a known spectral interval and a fixed-degree Chebyshev iteration provide normwise inner-error bounds. A stopping tolerance checked for one right-hand side, by itself, does not provide such an operator bound.

Theorem 6.2 (Perturbation guarantee)**.** *Let $p(z) = \sum_{j=0}^m c_j z^j$ be a residual polynomial selected above, and assume*

$$\left\| p(\widehat{\mathcal{B}}_\alpha) \right\|_2 \le \epsilon, \qquad \left\| \widetilde{\widehat{\mathcal{B}}} - \widehat{\mathcal{B}}_\alpha \right\|_2 \le \eta.$$

Choose $R \ge \max\{ \left\| \widehat{\mathcal{B}}_\alpha \right\|_2, \left\| \widetilde{\widehat{\mathcal{B}}} \right\|_2 \}$ and define

$$\mathcal{L}_p(R) = \sum_{j=1}^m j |c_j| R^{j-1}. \tag{6.4}$$

Then

$$\left\| p(\widetilde{\widehat{\mathcal{B}}}) \right\|_2 \le \epsilon + \eta \mathcal{L}_p(R) =: \widetilde{\epsilon}. \tag{6.5}$$

Let $\psi(z) = (1 - p(z))/z$ and $\widetilde{\mathcal{Q}} = \psi(\widetilde{\mathcal{B}})\widetilde{M}$. If $\widetilde{\epsilon} < 1$, then

$$\left\| I - D_\alpha \widetilde{\mathcal{Q}} \mathcal{A} D_\alpha^{-1} \right\|_2 \le \widetilde{\epsilon} < 1.$$

Thus fixed residual correction contracts the error in the D_α norm, and GMRES on the scaled left-preconditioned system has relative residual at most $\widetilde{\epsilon}^k$.

Proof. For any two matrices X, Y, $X^j - Y^j = \sum_{i=0}^{j-1} X^i (X - Y) Y^{j-1-i}$. The assumed norm bounds therefore imply $\|p(X) - p(Y)\|_2 \le \eta \mathcal{L}_p(R)$. Apply this with $X = \widetilde{\widehat{\mathcal{B}}}$ and $Y = \widehat{\mathcal{B}}_\alpha$. The exact polynomial identity $\widetilde{\mathcal{Q}}\mathcal{A} = I - p(\widetilde{\widehat{\mathcal{B}}})$ proves the final norm bound. Residual correction and the GMRES estimate follow as in theorem 5.2. □

Remark 6.3 (Variable inner applications). For a sequence of maps Q_k satisfying

$$\left\| I - D_\alpha Q_k \mathcal{A} D_\alpha^{-1} \right\|_2 \le \epsilon_k,$$

the consistent residual-correction iteration $x_{k+1} = x_k + Q_k(b - \mathcal{A}x_k)$ satisfies

$$\|D_\alpha(x_* - x_k)\|_2 \le \left(\prod_{j=0}^{k-1} \epsilon_j \right) \|D_\alpha(x_* - x_0)\|_2 .$$

This follows by applying the norm bound at every step. Flexible GMRES [8] is an appropriate practical option for changing inner applications. The fixed-matrix polynomial proof above is not, by itself, a convergence proof for arbitrary flexible GMRES applications. Sharper variable-preconditioning estimates remain a separate task.

7 Parameter selection

Suppose positive spectral intervals for U and T are known:

$$0 < u_- \le \sigma(U) \le u_+, \qquad 0 < t_- \le \sigma(T) \le t_+,$$

where the notation means interval inclusion. Bounds based on wider valid intervals are also permitted. For $0 < a \le b$, let

$$\theta_{[a,b]}(\alpha) = \max\left\{\left|\frac{\alpha - a}{\alpha + a}\right|, \left|\frac{\alpha - b}{\alpha + b}\right|\right\}.$$

Proposition 7.1 (Two candidates for the contraction bound)**.** *If $u_- > 0$, the product $\theta_{[u_-,u_+]}(\alpha)\theta_{[t_-,t_+]}(\alpha)$ attains its global minimum at one of*

$$\alpha_U = \sqrt{u_- u_+}, \qquad \alpha_T = \sqrt{t_- t_+}. \tag{7.1}$$

If U is singular, $\vartheta_\alpha(U) = 1$ and the exact product bound q_α is minimized by $\alpha_T = \sqrt{\lambda_{\min}(T)\lambda_{\max}(T)}$.

Proof. Set $x = \log\alpha$, $c_{a,b} = \frac{1}{2}\log(ab)$ and $w_{a,b} = \frac{1}{2}\log(b/a)$. Direct calculation yields

$$\theta_{[a,b]}(e^x) = \tanh\left(\frac{w_{a,b} + |x - c_{a,b}|}{2}\right).$$

Outside the interval joining the two centers, the product decreases toward that interval from the left and increases away from it on the right. Between the centers, each argument of tanh is affine. The function $y \mapsto \log\tanh(y/2)$ is concave for $y > 0$: its derivative is $1/\sinh y$ and its second derivative is $-\cosh y/\sinh^2 y < 0$. The logarithm of the product is therefore concave between the centers, so a minimum occurs at an endpoint. If an interval degenerates to a point and the product vanishes at its center, that point is already a global minimizer. This also handles zero factors. If U is singular, its Cayley transform has the eigenvalue 1, while all its eigenvalues have modulus at most 1. Minimizing the remaining single factor gives the geometric mean of the extreme eigenvalues of T. □

The proposition minimizes a sufficient convergence bound, not elapsed time. A practical choice should also account for Γ_α, ellipse geometry, the degree selected by (5.10), and the cost of the two SPD solves. For example, an implementation may evaluate the two candidates and a small neighboring set, then minimize a measured cost model at a fixed target contraction. Obtaining useful bounds for U without forming T^{-1} is part of the implementation problem. The bound $0 \preceq U \preceq \|W\|_2^2 / \lambda_{\min}(T)\, I$ is always available when the indicated norm and lower bound are known, but may be pessimistic.

8 Numerical experiments

The numerical experiments were performed in Python 3.12.14 using NumPy 2.3.5, SciPy 1.17.0 and Matplotlib 3.10.8 on Linux. All computations used a single BLAS thread, and the random seed was fixed at 20261031. The test matrices were generated from the definitions given below, without external datasets.

Computational work is assessed by counting matrix actions and scalar orthogonalization inner products separately. For each sparse matrix, the same block preconditioner is reused across the polynomial degrees considered. Reported solution times are medians of three runs and exclude preconditioner setup, whose cost is recorded separately. The count N_B includes all applications of $\widehat{\mathcal{B}}_\alpha$ during the iterative solve, the final GMRES residual verification and

Table 1: Dense family, $n = 48$. Reduced polynomial bounds at $\ell = 8$. The ellipse column includes the Crouzeix–Palencia factor for $\theta > 0$; the interval case at $\theta = 0$ uses constant 1.

θ	q_α	b_α	$\max \lvert \operatorname{Im} \lambda \rvert$	disk bound	ellipse bound
0.00	0.669	0.000e+00	0.000e+00	4.03e-02	9.47e-04
0.02	0.670	7.580e-03	8.539e-07	4.05e-02	3.81e-03
0.10	0.677	3.701e-02	1.369e-02	4.41e-02	1.74e-02
0.30	0.719	9.899e-02	6.328e-02	7.17e-02	1.24e-01
0.70	0.782	1.954e-01	1.558e-01	1.40e-01	4.37e-01
1.20	0.802	2.697e-01	2.290e-01	1.72e-01	7.92e-01

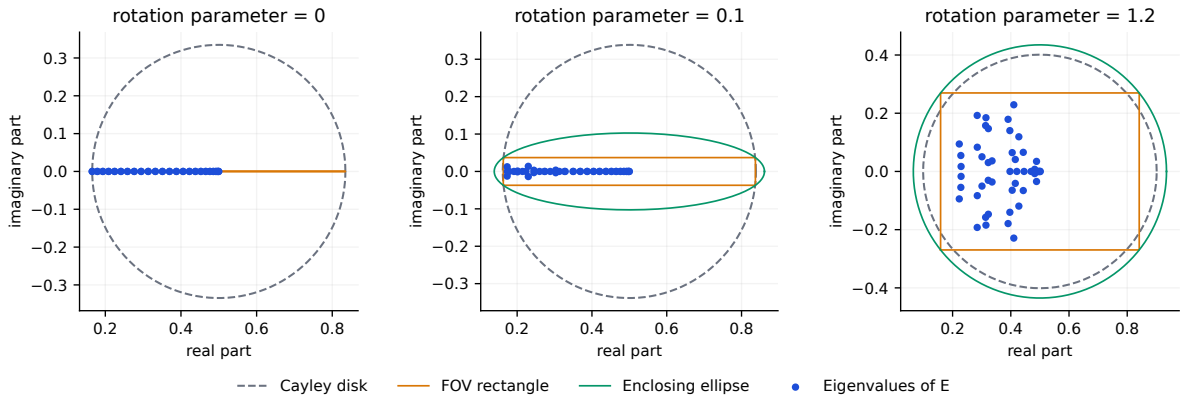


Figure 1: Reduced eigenvalues, Cayley disk, numerical-range rectangle and an enclosing ellipse for three members of the rotation family. Numerical ranges themselves are not plotted; the rectangle encloses them.

polynomial solution recovery. Each application consists of one multiplication by $\mathcal{A}$, one block preconditioner application and diagonal scaling. Independent evaluations of the physical and scaled residuals after solution recovery are excluded from both the reported solution times and N_B.

Additional numerical checks cover the Cayley-transform identity, the commutator estimate, the full-block residual-polynomial bound and the polynomial approximate-inverse recurrence, including cases with singular W. The counterexample is checked through its characteristic polynomial, and the two-candidate parameter rule is compared with logarithmic parameter sweeps.

8.1 Spectral transition at fixed constituent spectra

Let $n = 48$, $T = \operatorname{diag}(t_i)$ with t_i geometrically spaced from 0.1 to 10, and $D_W = \operatorname{diag}((-1)^i t_i)$, with alternating signs. Generate a real skew-symmetric matrix K from the stated seed, scale it so that $\|K\|_2 = 1$, and set

$$Q_\theta = e^{\theta K}, \qquad W_\theta = Q_\theta D_W Q_\theta^T, \qquad \alpha = 1.$$

The spectra of T and W_θ are fixed, while their relative eigenvectors change. At $\theta = 0$, $U = T$ and the reduced block is symmetric. For $\theta > 0$ it may acquire nonreal eigenvalues.

Table 1 and figure 1 show the transition from a real spectrum to a complex cloud. The ellipse bound improves the disk estimate for weak rotation, while the disk estimate is preferable for the larger rotations in this experiment. The selection rule chooses the smaller bound, rather than assuming an ellipse is always beneficial. In particular, the eigenvalues alone are a less demanding target than the numerical range.

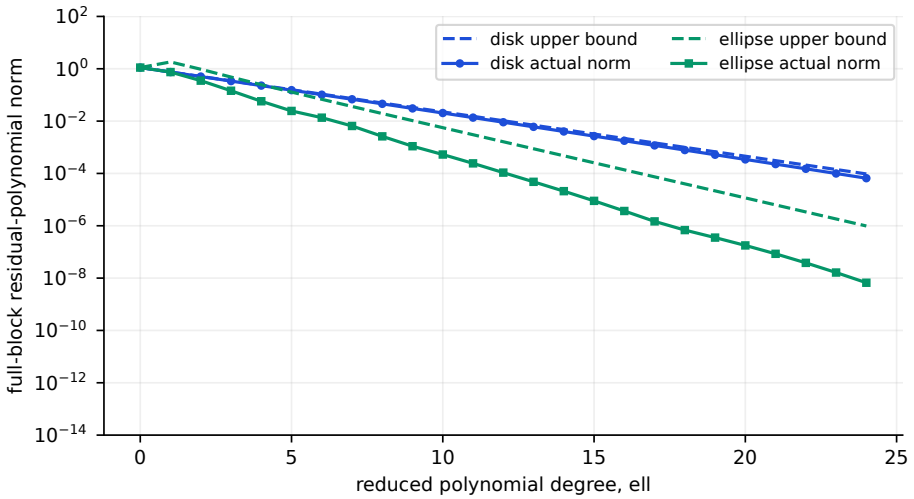


Figure 2: Full-block residual-polynomial norms and upper bounds for $\theta = 0.1$. The exponent is the reduced degree ℓ; the full residual polynomial has degree $\ell + 1$. Values near machine precision indicate the floating-point evaluation floor.

For $\theta = 0.1$, figure 2 compares actual full-block residual polynomial norms with the estimates of theorems 4.1 and 5.1. The dense implementation computes a_α, b_α explicitly and searches 240 admissible values of A for each degree. These spectral diagnostics are intentionally affordable only for the small dense family; their cost is not hidden in a claimed scalable solver.

8.2 Sparse shifted-Laplacian systems and work accounting

For a $g \times g$ grid, let K_g be the unscaled five-point Dirichlet Laplacian, with one-dimensional stencil $(-1, 2, -1)$, and set

$$W = K_g - 2I, \qquad T = \operatorname{diag}\left(0.1 + 0.45\{1 + \sin(2\pi x_i)\sin(2\pi y_i)\}\right), \tag{8.1}$$

where x_i, y_i are interior grid coordinates. The matrix W is symmetric indefinite, and the spatially varying diagonal T does not commute with it. We use $\alpha = 1$, sparse LU for H_α, and the exact diagonal inverse of S_α. This is an algebraic scaling family; the unscaled stencil and fixed shift do not define a fixed-frequency PDE mesh-refinement study. The experiment examines polynomial work tradeoffs.

The physical right-hand side is $b = \mathcal{A}x_*$ with $(x_*)_j = \sin(0.13j) + 0.25\cos(0.07j)$. GMRES is unrestarted, starts from zero and uses two modified Gram–Schmidt passes. The stopping target for the scaled residual is 10^{-11}. We compare the base matrix $\widehat{\mathcal{B}}_\alpha$ with right polynomial preconditioning of disk degrees $\ell = 2$ and 5. The transformed unknown is recovered after GMRES, and the physical residual is explicitly recomputed.

The polynomial reduces outer iterations and orthogonalization dot products, but requires more constituent block-preconditioner applications. The reported single-process timings are small, hardware-dependent observations, and do not establish a consistent speedup. A reduction in scalar dots is also not a direct measurement of distributed global reductions, since implementations may fuse or pipeline them. The intended next benchmark is a distributed implementation with measured communication and equal physical-residual targets.

8.3 Fixed inexact subsolves

For the dense rotation family with $n = 24$ and $\theta = 0.1$, replace both SPD inverses by fixed Chebyshev approximate inverses with the indicated number of steps. Exact numerical spectral

Table 2: Sparse systems: $n = g^2$ complex unknowns and $2n$ real unknowns. N_B includes the final GMRES residual verification and polynomial solution recovery. Dots count scalar inner products in the two orthogonalization passes; vector-norm operations are not included.

g	ℓ	outer	N_B	dots	physical residual	solve (s)
16	0	20	21	420	4.9e-12	0.0037
16	2	8	29	72	1.3e-12	0.0037
16	5	6	47	42	1.2e-12	0.0053
24	0	21	22	462	4.0e-12	0.0058
24	2	8	29	72	4.5e-12	0.0053
24	5	6	47	42	1.3e-12	0.0074
32	0	21	22	462	9.2e-12	0.0121
32	2	8	29	72	1.3e-11	0.0066
32	5	6	47	42	2.1e-12	0.0115

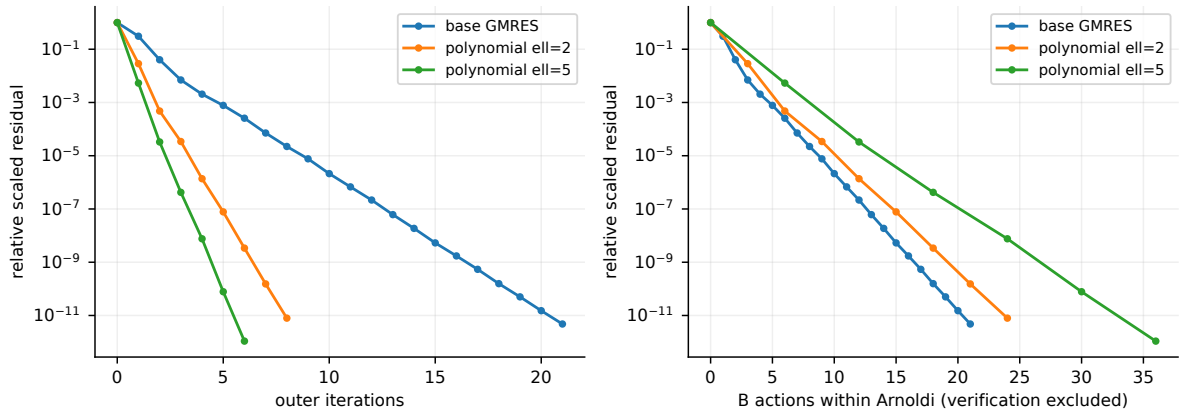


Figure 3: Sparse 32×32 grid: convergence against outer iterations and constituent $\mathcal{B}_\alpha$ actions within Arnoldi. Final verification and recovery actions are included in table 2, not the horizontal axis of the right panel.

endpoints of the small dense SPD matrices define the Chebyshev intervals. We evaluate the full disk residual polynomial at $\ell = 3$ and compare with theorem 6.2. Here $\delta_X = \|I - XM_X\|_2$ and η is the measured scaled preconditioned-matrix difference; the table isolates the polynomial perturbation theorem rather than the additional bound in lemma 6.1.

Table 3 demonstrates the effect of underresolved inner solves: the actual residual-polynomial norm can exceed 1 even though each inner SPD inverse is approximated by a convergent Chebyshev process. More inner steps eventually recover the exact-case behavior. The coefficientwise Lipschitz bound is conservative, especially for a high-degree polynomial; sharper recurrence-level perturbation estimates are therefore a useful extension.

9 Conclusions

A Cayley-transform representation provides spectral and convergence bounds for the relaxed block preconditioner without a commutativity assumption. The corrected enclosure permits nonreal eigenvalues while placing the nontrivial spectrum in a disk contained in the open right half-plane. Commutator estimates further control the numerical range and departure from normality. An explicit block-polynomial identity accounts for the coupling block and the unit eigenvalues, allowing reduced polynomial estimates to be transferred to the full system. This identity leads to a polynomial approximate inverse selected from disk and Chebyshev

Table 3: Fixed inexact subsolves. The final two columns are the actual full residual-polynomial norm and the perturbation bound $\Gamma_\alpha q_\alpha^3 + \eta \mathcal{L}_p(R)$.

steps	δ_S	δ_H	η	actual norm	upper bound
2	5.03e-01	9.92e-01	9.25e+00	1.09e+01	2.98e+05
4	1.45e-01	9.68e-01	8.36e+00	1.10e+01	1.91e+05
8	1.06e-02	8.80e-01	8.78e+00	1.62e+01	2.31e+05
16	5.63e-05	6.32e-01	6.37e+00	9.60e+00	6.95e+04
32	1.58e-09	2.50e-01	2.52e+00	1.51e+00	2.77e+03
64	5.00e-15	3.22e-02	3.24e-01	3.59e-01	6.71e+01
128	6.66e-15	5.19e-04	5.23e-03	3.39e-01	1.43e+00
256	2.35e-14	1.34e-07	1.35e-06	3.39e-01	3.54e-01

constructions, together with parameter-selection and fixed-inexact perturbation guarantees.

The numerical experiments support the predicted spectral transition and operator-norm estimates. They also show why outer iteration counts should be interpreted together with constituent preconditioner applications and orthogonalization work. For the tested families, polynomial acceleration reduces outer iterations and scalar orthogonalization products at the cost of additional block actions. Its elapsed-time benefit therefore depends on the relative costs of those operations.

Further work concerns scalable upper bounds for the numerical-range enclosures, sharper recurrence-level perturbation estimates, and uniform control of coupling and norm-equivalence constants for specified discretization families. Distributed experiments with scalable inner solvers would determine when the reduction in outer orthogonalization offsets the additional polynomial work.

Statements and Declarations

Competing Interests and Funding The author declares no competing interests. This research received no external funding.

References

[1] Z.-Z. Bai, G. H. Golub, and M. K. Ng, Hermitian and skew-Hermitian splitting methods for non-Hermitian positive definite linear systems, *SIAM Journal on Matrix Analysis and Applications* **24** (2003), 603–626. doi:10.1137/S0895479801395458.

[2] W. Bao and S. Miao, A modified block preconditioner for complex symmetric indefinite linear systems, *Journal of Applied Analysis and Computation* **14** (2024), 182–196. doi:10.11948/20230131.

[3] H. Chen and C. Greif, GMRES convergence analysis for nonsymmetric saddle-point systems when the field of values contains the origin, arXiv:2505.07156, version 2, 11 February 2026. doi:10.48550/arXiv.2505.07156.

[4] M. Crouzeix and A. Greenbaum, Spectral sets: numerical range and beyond, *SIAM Journal on Matrix Analysis and Applications* **40** (2019), 1087–1101. doi:10.1137/18M1198417.

[5] M. Crouzeix and C. Palencia, The numerical range is a $(1+\sqrt{2})$-spectral set, *SIAM Journal on Matrix Analysis and Applications* **38** (2017), 649–655. doi:10.1137/17M1116672.

[6] M. Embree, R. B. Morgan, and H. V. Nguyen, Weighted inner products for GMRES and GMRES-DR, *SIAM Journal on Scientific Computing* **39** (2017), S610–S632. doi:10.1137/16M1082615.

[7] A. Greenbaum, V. Pták, and Z. Strakoš, Any nonincreasing convergence curve is possible for GMRES, *SIAM Journal on Matrix Analysis and Applications* **17** (1996), 465–469. doi:10.1137/S0895479894275030.

[8] Y. Saad, A flexible inner-outer preconditioned GMRES algorithm, *SIAM Journal on Scientific Computing* **14** (1993), 461–469. doi:10.1137/0914028.

[9] Y. Saad and M. H. Schultz, GMRES: A generalized minimal residual algorithm for solving nonsymmetric linear systems, *SIAM Journal on Scientific and Statistical Computing* **7** (1986), 856–869. doi:10.1137/0907058.

[10] H.-Y. Wu, An efficient block preconditioner for a class of complex symmetric linear systems, *Communications on Applied Mathematics and Computation* (2026), published online 21 August 2026. doi:10.1007/s42967-026-00604-8.

[11] J.-H. Zhang and H. Dai, A new block preconditioner for complex symmetric indefinite linear systems, *Numerical Algorithms* **74** (2017), 889–903. doi:10.1007/s11075-016-0175-y.